ACS Sustainable Chemistry & Engineering

Research Article

pubs.acs.org/journal/ascecg

Novel Hemicellulose–Chitosan Biosorbent for Water Desalination and Heavy Metal Removal

Ali Ayoub, Richard A. Venditti,* Joel J. Pawlak, Abdus Salam, and Martin A. Hubbe

Department of Forest Biomaterials, College of Natural Resources, North Carolina State University, Raleigh, North Carolina 27695-8005, United States

Supporting Information

ABSTRACT: Hemicellulose material is an abundant and relatively under-utilized polymeric material present in lignocellulosic materials. In this research, an alkaline treatment was applied to pinewood (PW), switchgrass (SG), and coastal bermuda grass (CBG) in order to extract hemicelluloses to subsequently produce a novel biosorbent. Alkaline extraction at 75 °C recovered 23% of the biomass as a predominantly hemicellulose material with a number average degree of polymerization of ~450. These hemicelluloses were grafted with penetic acid (diethylene triamine pentaacetic acid, DTPA) and were then cross-linked to chitosan. The effects of hemicellulose–DTPA concentration, reaction time, and temperature of reaction with chitosan on the resulting salt (sodium chloride, NaCl) uptake and weight loss in saline solutions were determined. A maximum salt uptake for the materials was ~0.30 g/g of foam biosorbent. The foam biosorbent was characterized by FT-IR spectra, porosity, and dynamic mechanical analysis. Batch adsorption equilibrium results suggest that the adsorption process for salt follows a second-order kinetic model. The hemicellulose-DTPA-chitosan foam biosorbent had uptakes of 2.90, 0.95, and 1.37 mg/g of Pb^{2+}, Cu^{2+}, and Ni^{2+} ions, respectively, from aqueous medium at initial concentrations of 5000 PPB at pH 5. The cross-linked hemicellulose–DTPA–chitosan material has good potential for environmental engineering applications.

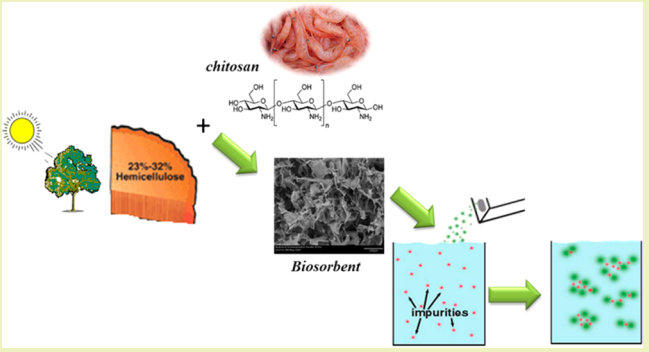

KEYWORDS: *Hemicellulose extraction, Chitosan, Desalination, Heavy metals, Penetic acid*

INTRODUCTION

Limitations to the availability of clean water are recognized currently as a global human health threat. At the current growth rates, the population will be consuming 90% of the available fresh water by 2025.[1] Moreover, the increasing level of toxic ionic species that are charged into the environment as industrial wastes represents a serious threat to human health, living resources, and ecological systems.

While techniques to remove salt from water have existed for centuries and the recent years have seen significant advances in desalination technology, desalinated water remains considerably more expensive and energy-intensive than fresh water from existing sources.[2−4]

On the other hand, activated carbon has been the most popular material for the removal of heavy metals and other species.[5,6] However, the high cost of this material makes its application less economically attractive in some low-cost applications for industrial scale.[7]

To reduce the operational costs, the search for alternative materials for environmental engineering has intensified in recent years.[8] The technology for the purification of water can benefit from the utilization of renewable biomaterials with performance properties comparable to petroleum-based synthetic materials.

Hemicellulose has excellent potential for this application.[9−11] Hemicelluloses are branched polymers of low molecular weight with a degree of polymerization in the range of 80−450.[12] In the pulp and papermaking process, on the order of 100s of millions of tons of hemicellulose may be available worldwide annually. The chemical modification of hemicelluloses presents a means for preparing materials with unique properties that can increase value and utility of these biopolymers.[13−15] One such area of application is super-absorbent hydrogels.[10,16] Hydrogels have attracted significant attention in biomedical applications because of their high liquid up-take and their stimuli-responsive swelling–deswelling capabilities without disintegration. They owe their mechanical stability during swelling to cross-links introduced between the macromolecular chains that allow for flexibility but sufficient strength.[11,17,18]

Chitosan is also a renewable biopolymer and has been widely used to prepare natural hydrogels.[10,11,19] However, hydrogels based on chitosan generally lack mechanical stability unless they are cross-linked and/or reinforced by suitable com-

Received: December 17, 2012
Revised: May 7, 2013
Published: June 18, 2013

ACS Publications © 2013 American Chemical Society

pounds.[9,20] Gabrielii et al.[9] studied chitosan hydrogels that contained xylan for reinforcement.

In order to utilize biopolymers to remove impurities from water, it is important to strongly bond ionic species to the adsorbent surface. The surfaces of biopolymer adsorption materials may be covered by functional groups such as amine in the case of chitosan. Bonds between these simple surface groups and metal cations, however, are not usually strong. Therefore, surface functionalization with high affinity binding such as diethylene triamine pentaacetic acid (DTPA) form very strong chelates with ionic species and may produce materials with excellent metal binding properties.[21,22]

In this study, hemicellulose isolated from wood and grasses were evaluated with chitosan for use as a foam material that also possesses desalination and uptake of heavy metals characteristics. The present investigation details the synthesis and characterization of such materials and demonstrates their capabilities to adsorb salts and metal ions. A kinetic model of salt adsorption on the foams was developed to fit time and concentration of salt adsorption data adequately. The ability of the novel gel materials to maintain their water-swollen condition in the presence of salt and also their unusual ability to take up salt from an aqueous environment are discussed in terms of the behavior of polyelectrolyte complexes.

EXPERIMENTAL SECTION

Materials. Switchgrass (SG) and coastal bermuda grass (CBG) were harvested in August 2011 from the Cherry Research Farm of the State Department of Agriculture in Goldsboro, North Carolina, U.S.A. The materials were stored indoors and allowed to equilibrate for 4 weeks prior to use. Moisture content of the air-dried materials was measured by oven drying at 105 °C until constant weight was achieved. Pinewood (PW) from North Carolina was used in this study as well. Hemicellulose was isolated from different types of biomass by an alkaline extraction method (Figure S1, pages S1 and S4, Supporting Information). The chitosan (medium molecular weight, degree of deacetylation 75−85%), CAS registry number 9012-76-4, was purchased from Sigma−Aldrich, St. Louis, MO. The following reagent grade chemicals were also used: sodium hypo-phosphite (SHP), CAS registry number 123333-67-5; DTPA, CAS registry number 77-92-9; sodium chloride, and acetic acid, from Fisher Scientific, Fair Lawn, NJ. Whatman filter paper (quantitative number 4, 110 mm diameter) from Whatman International Ltd., Maidstone, England, and deionized water was used throughout.

Compositional Analysis. The moisture contents of the biomass feedstocks were determined with an infrared moisture analyzer, Mettler PM100, Toledo, OH, U.S.A. Hemicellulose was determined by high performance liquid chromatography (HPLC) analysis of monomeric sugars (glucose, xylose, galactose, and arabinose) as described in our previous work.[23]

Gel Permeation Chromatography (GPC). The molecular weights of acetylated hemicellulose were determined by GPC. Measurements were carried out with a Waters GPC 510 pump equipped with UV and RI detectors using tetrahydrofuran (THF) as the eluent at a flow rate of 0.7 mL/min at room temperature as described in our previous paper.[23] Two ultrastyragel linear columns linked in series (Styragel HR 1 and Styragel HR 5E) were used for the measurements.

Modification of Hemicellulose with DTPA in Solution. A modified procedure[10] that has been demonstrated for citric acid and hemicellulose materials was utilized herein. In a 250 mL round-bottomed flask, 1 g of hemicellulose was treated with 0.05 M of DTPA solution (pH 3.9) in 100 mL in the presence of SHP (10% by weight on DTPA). The SHP is a catalyst for the reaction. The flask was equipped with a reflux condenser and immersed in an oil bath. The reaction mixture was stirred using a magnetic stirrer for 2.5 h at 110 °C (optimizing condition), followed by cooling in ambient conditions to room temperature (1 h). The reaction mixture (clear solution) was then slowly added to 50 mL of isopropanol in a glass beaker resting in a water−ice bath, and a white precipitated solid is formed. The solid is collected by filtration on filter paper using house vacuum and the product air-dried.

Cross-Linking between Hemicellulose−DTPA and Chitosan. A chitosan solution was prepared by adding 1 g of chitosan to a mixture of 99 mL of water and 1 mL of glacial acetic acid. The chitosan solution was added to 100 mL of a 1% hemicellulose−DTPA solution in a 250 mL round-bottomed flask. The reaction mixture was stirred using a magnetic stirrer with the flask placed in an oil bath at 110 °C for 2.5 h (optimizing condition). Water evaporation was controlled by the use of a condenser. Following the reaction, the mixture was cooled to room temperature (1 h), and the hemicellulose−DTPA−chitosan foam biosorbent product was then formed by freeze drying.

FT-IR Analysis. The spectra were recorded on a NEXUS 670 FTIR spectrophotometer using a KBr disc containing 10% finely ground sample particles. All the spectra were obtained by accumulation of 256 scans, with resolution of 4 cm^{-1} at 400−4000 cm^{-1}.

Scanning Electron Microscopy. The morphological characterization and elemental analysis (energy dispersive X-ray spectroscopy, EDAX) of hemicellulose−DTPA−chitosan was performed on images acquired using a scanning electron microscope (SEM), Hitachi S-3200N, as described in our previous work.[10]

Liquid Absorption Analysis. The sample (approximately 20 mg, preweighed) was soaked in 50 mL distilled water for 1 h. An aluminum foil filter circle with holes of approximately 0.5 mm was placed into a Buchner funnel attached to house vacuum. The contents of the dish were poured onto the filter foil. The dish was rinsed with about 15 mL of additional DI water, and this water was also poured into the funnel. Another foil without holes was placed on top of the sample, and a mass of 5500 g was applied over an area of 20 cm^2 for 15 min. This equates to a pressure of 0.30 kPa. Once water removal ceased, the sample was lifted off the foil aluminum circle and then weighed to determine water absorption per gram of sample. Absorption and weight loss with an aqueous NaCl solution (concentration: 0.3 and 0.9%) was investigated similarly.

Salt Adsorption Experiments. Samples were immersed in known salt concentration solutions in batch reactors within a temperature-controlled water bath and removed after predetermined times. Excess water was removed using the process outlined in the liquid absorption analysis experimental section. Gravimetric analysis of the resulting material before and after drying at 105 °C was used to determine salt adsorbed. Considerations were made to subtract extraneous salt that existed in free liquid in the pores of the samples.

Dynamic Mechanical Analysis. This was performed with a DMA Model 2980 (TA, Inc., New Castle, DE, U.S.A.) in the film-tension mode. Sample dimensions were approximately 30 mm length, 10 mm width. and a 3.5 mm thickness. Samples were heated from −50 to 200 °C at 2 °C/min (static strain of 0.67%, 20 μm amplitude, 1 Hz). Each sample was measured for length, width, and thickness before mounting.

Heavy Metal Removal Test. This was measured by inductively coupled plasma optical emission spectrometry (ICP-OES) available in the Soil Science Department at North Carolina State University, Raleigh, NC, U.S.A. The adsorption of heavy metal such as nickel(II), copper(II), and lead(II) mg/g were studied at different pH values using switchgrass hemicellulose−DTPA−chitosan biosorbent at initial metal ion concentrations of 5000 PPB and 100 PPB. Adjustment of pH was made with 0.1 N HCl and 0.1 N of NaOH solutions.

RESULTS AND DISCUSSION

Extraction of Hemicelluloses. One objective of this study was to extract hemicellulose from readily available sources such as pinewood (PW), switchgrass (SG), and coastal bermuda grass (CBG) in a simple way for new applications. Softwoods like pine, unlike hardwood, have higher lignin content in the cell wall resulting in a high degree of entrapment of the polysaccharides. Therefore, these polysaccharides are difficult

to be extracted by solvent extraction. In this study, lignin was removed using concentrated NaOH and ethanol, and the resulting holocellulose solids were then extracted using 10% NaOH to provide a filtrate rich in hemicellulose (Pages S1 and S4, Supporting Information).

The precipitates of the filtrate after the addition of ethanol were collected with a yield of hemicellulose of 23% of dry biomass for pine comparable to another report on southern pine of 21%.[25] The yields of SG and CBG of 26.39 and 29.1 are quite similar to those in literature of NREL, 24.4 and 24.8%, respectively.[25] Hemicelluloses are expected to be more readily extracted in grasses and hardwoods than softwoods due to different lignin content and structure.[26]

The neutral monosaccharide compositions of the three biomass samples are given in Table 1, with xylose being the predominant sugar in all three materials. The weight-average (M_w) was 79,800, 85,710, and 83,200 g mol^{-1} for PW, SG, and CBG, respectively (Table 1). Sun et al.[27] have shown the hemicelluloses extracted from the lignified residue of sugar beet pulp with 8% NaOH and ethanol at 15 °C for 16 h had a similar molecular weight of about 88,000 g mol^{-1}. Another study by Gabriellii et al.[9] has shown the hemicellulose extracted from aspen wood has as well similar molecular weight of about 73,000 g mol^{-1}.

Table 1. Yield and relative content of neutral sugars in the hemicellulose from grasses and pinewood based on 100g initial biomass OD and its molecular weight determined by GPC

	pinewood	switchgrass	coastal bermuda grass
	% on initial OD biomass		
arabinose	2.2	3.1	4.4
galactose	1.4	0.8	1.9
glucose	1.3	1.0	0.8
mannose	4.7	0.2	0
xylose	13.5	21.8	22.0
total yield (hemicellulose)	23.1	26.39	29.1
molecular weight for acetylated samples with GPC, THF as the eluent			
M_w (g mol^{-1})	79,800	85,710	83,200
M_n (g mol^{-1})	20,050	20,670	20,830
PD	3.9	4.2	4
	beet pulp hemicellulose[26]		
M_w (g mol^{-1})	88,850		
M_n (g mol^{-1})	10,650		
PD	8.34		
	hemicellulose from aspen wood[9]		
M_w (g mol^{-1})	73,100		
M_n (g mol^{-1})	48,000		
PD	1.52		

Modification of Hemicellulose with DTPA in Solution. A simplified reaction path expected for the reaction of DTPA with the hemicelluloses is shown in Figure S2 of the Supporting Information. The DTPA addition increased the carboxyl content of the carbohydrate as expected. The degree of substitution (DS) was calculated from titration as described elsewhere.[15]

The DS of the hemicellulose using SG of 1.39 was somewhat higher than coastal Bermuda grass or pinewood (Table S1, Supporting Information). It was observed that the use of the catalyst SHP increased the degree of substitution of the chemical reaction and yield relative to reaction without the catalyst (data not shown). This can be explained because the sodium hypophosphite catalyzer enhances production of the anhydride functionality formed from the carboxyl group of DTPA.

Analysis of the FTIR data in Figure S3 of the Supporting Information for hemicellulose showed an absorption band in the 1200−1000 cm^{-1} region typical for xylose. This region is dominated by ring vibrations overlapped with stretching vibrations of C−OH side groups and the C−O−C glycosidic bond vibration. A strong broad peak due to hydrogen-bonded hydroxyls appears at 3414 cm^{-1}. In the DTPA spectrum, it is possible to observe a C═O band centered at 1712 cm^{-1} due to carboxylic acid. When hemicellulose is reacted with DTPA, peaks appear at around 1600, 1480, 140, and 1230 cm^{-1} and between 1280 and 1050 cm^{-1}, attributable to the characteristic stretching band of carboxylate and esters groups. Also, the decrease in the peak at 3414 cm^{-1} qualitatively indicates the conversion of hydroxyl to esters. New peaks appear at 3030 and 2780 cm^{-1} attributable to the OH of carboxylic acids.

Hemicellulose−DTPA and Chitosan Absorption Properties. The water and saline absorption properties of the hemicellulose−DTPA (from PW, SG, and CBG, separately) and chitosan material before and after reaction at 1:1 mass ratio (t = 2.5 h, T = 110 °C) are shown in Table 2. The results of the HC−DTPA−CS are similar for all three hemicellulose sources. The HC−DTPA−CS materials have significantly higher water and saline absorption and lower weight loss than the individual components alone. The decrease in weight loss indicates that the cross-linking occurring during the HC−DTPA reaction with CS develops a more complete network and thus less dissolution of the foam material. Further, a negative weight loss for HC−DTPA−CS after exposure to saline solution indicates that the foam is strongly absorbing salt from the solution. Because the behavior of the HC−DTPA−CS material for all three hemicellulose sources was so similar, further detailed inspection of the SG hemicellulose alone was carried out in the following research. However, this is unlike a conventional

Table 2. Properties of Hemicellulose−DTPA−Chitosan and Others Materials[a]

	weight loss (%) at 1 h		water and saline absorption (g/g)		
sample	water	NaCl (0.3%)	water	NaCl (0.3%)	NaCl (0.9%)
hemicellulose, SG	13 ± 3	9 ± 2	1 ± 0	1 ± 0	2 ± 0
hemicellulose, PW	10 ± 1	7 ± 1	1 ± 0	1 ± 0	2 ± 0
hemicellulose, CBG	13 ± 1	9 ± 2	1 ± 0	1 ± 0	2 ± 0
chitosan, CS	49 ± 2	43 ± 1	7 ± 0	8 ± 0	9 ± 0
HC−DTPA, SG	17 ± 1	13 ± 2	4 ± 1	3 ± 2	5 ± 1
HC−DTPA−CS, SG	9 ± 2	−7 ± 1	23 ± 1	23 ± 2	27 ± 2
HC−DTPA−CS, PW	10 ± 2	−5 ± 2	20 ± 1	19 ± 3	27 ± 2
HC−DTPA−CS, CBG	9 ± 2	−7 ± 0	23 ± 0	23 ± 1	28 ± 4
commercial cellulose foam	55 ± 1	50 ± 1	2 ± 0	2 ± 0	3 ± 0

[a]Average and standard deviation are reported for three tests of each sample. [b]Reaction conditions: hemicellulose−DTPA to chitosan mass ratio 1:1, t = 2.5h, T = 110 °C.

super-absorbent, which absorbs less saline solution than pure water. This increased saline absorption was also accompanied by other changes in the degree of weight loss of the foam when compared to commercial super-absorbents.

Effect of Reaction Time. A schematic of the reaction between SG hemicellulose–DTPA and chitosan is shown in Figure S4 of the Suppporting Information. The reaction time (0.5–2.5 h) was investigated with the following held constant: hemicellulose–DTPA/chitosan ratio of 1:1, pH 3.9, and T = 110 °C. The FT-IR spectra of hemicellulose, hemicellulose–DTPA, and hemicellulose–DTPA–chitosan are shown in Figure 1. Analysis of the FT-IR data for the foam showed a

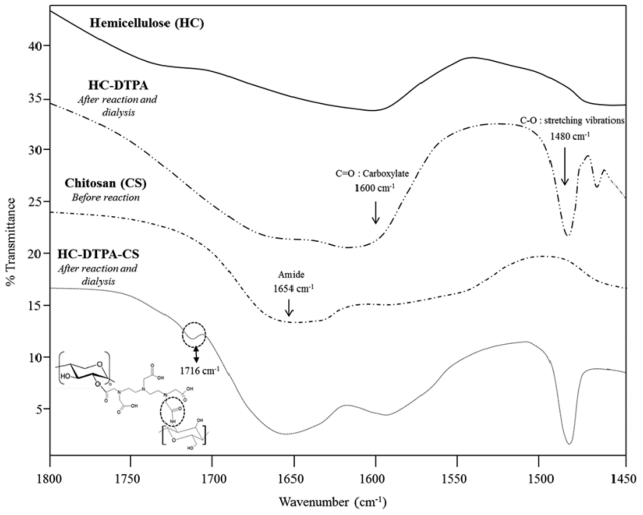

Figure 1. FTIR spectra of hemicellulose, hemicellulose–DTPA, chitosan, and hemicellulose–DTPA–chitosan after reaction.

new peak at 1716 cm^{-1}, attributable to the characteristic stretching band of carbonyl groups in an amide bond of hemicellulose DTPA cross-linked with chitosan.[24] This is in agreement with the hemicellulose–DTPA being linked to chitosan via reactions between amine groups of chitosan and carboxylic groups of hemicellulose–DTPA. This supports the notion that hemicellulose–DTPA and chitosan are covalently cross-linked to some extent.

SEM images reveal the structure of the hemicellulose–DTPA–chitosan foam as being a connected three-dimensional structure with a continuous connected open cell foam pore structure (Figure 2). The hemicellulose–DTPA–chitosan SEM images reveal a finer pore structure when compared to the hemicellulose–chitosan material.

The water and saline absorption increased with increasing reaction time for the materials (Table 3). Also, the weight loss decreases with reaction time, indicating a more completely cross-linked structure (Table 3). The strength of these products at reaction temperature 90 °C was very low, and the foam products collapsed when immersed in water. It is thought that the anhydride formation involved in the reaction is not sufficient at the lower temperature.

Effect of Hemicellulose–DTPA Concentration to Chitosan Ratio. To investigate the effect of the ratio of switchgrass hemicellulose–DTPA to chitosan, the concentration of switchgrass hemicellulose–DTPA was varied, and the amount of chitosan was fixed. It was determined from titration that the switchgrass hemicellulose-grafted DTPA had approximately 835 mequivalents per 100 g of material, and the chitosan had 525 mequivalents (amine) per 100 g of material. The effects of the ratio of hemicellulose–DTPA to chitosan on the absorption of the resulting foams are shown in Table 4. The water and saline absorption increases with increased hemicellulose–DTPA to chitosan ratio, in accordance with the increased hydrophilic carboxylic acid content.

Sodium chloride appears to form a complex with hemicellulose–DTPA–chitosan. This is evidenced by the conductivity of the saline solution before and after the soaking of the foam (Figure S5, Supporting Information. The decrease in conductivity indicates a decrease in sodium and chloride ion concentration in the solution. To further elaborate on the interaction of hemicellulose–DTPA–chitosan with the saline solution, the salt was detected in the foams by SEM/EDAX after an absorption equilibration experiment and drying the sample. A large number of nodules are noted in the SEM photomicrograph (Figure S6, Supporting Information). The EDAX spectrum of the small surface nodules indicates a high content of salt uptake.

Mechanical Properties. The dynamic mechanical analysis results related to the tensile modulus of switchgrass hemicellulose DTPA–chitosan foam and switchgrass–hemicellulose–chitosan blend are shown in Figure S7 of the Supporting Information. The storage modulus of hemicellulose–DTPA–chitosan foam was significantly higher than that of the hemicellulose–chitosan foam, and the tan delta (tangent of E′′/E′, where E is the elastic modulus) is lower, in agreement with increased cross-linking[44] of the hemicellulose–DTPA to chitosan relative to the hemicellulose to chitosan. Two

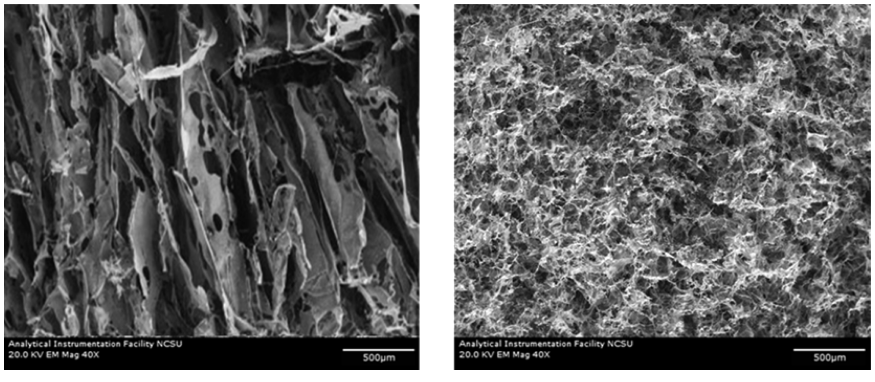

Figure 2. SEM images of a simple blend of switchgrass hemicellulose and chitosan foam (left) and hemicellulose–DTPA–chitosan foam-based materials after reaction (right).

Table 3. Effect of Reaction Time on the Properties of Foam Based on Switchgrass Hemicellulose−DTPA−Chitosan

HC−DTPA−CS reaction time (h) at T = 110 °C	apparent density (g/cm^3)	void fraction	weight loss (%), 1 h		absorption (g/g)	
			water	NaCl (0.3%)	water	NaCl (0.3%)
0.5	0.00930	0.9937	32 ± 4	27 ± 2	9 ± 1	10 ± 3
1	0.00939	0.9945	30 ± 3	27 ± 1	14 ± 2	10 ± 1
1.5	0.00956	0.9960	24 ± 1	15 ± 3	17 ± 2	19 ± 1
2	0.00969	0.9972	13 ± 1	−10 ± 2	22 ± 1	25 ± 3
2.5	0.00978	0.9980	8 ± 2	−24 ± 4	29 ± 3	34 ± 5

Table 4. Effect of Concentration Hemicellulose−DTPA on Properties of Foam Based on Switchgrass Hemicellulose−DTPA−Chitosan

ratio HC−DTPA:CS at T = 110 °C, t = 2.5hrs	apparent density (g/cm^3)	void fraction	absorption (g/g)	
			water	NaCl (0.3%)
0.2	0.00946	0.9951	8 ± 1	10 ± 2
0.5	0.00959	0.9963	7 ± 2	10 ± 1
0.8	0.00968	0.9971	18 ± 2	21 ± 1
1	0.00978	0.9980	29 ± 3	34 ± 4
1.2	0.00972	0.9975	32 ± 3	34 ± 3

[a]Reaction time =2.5 h, T = 110 °C. [b]Hemicellulose extracted from SG, M_w = 85,710 g/mol

transitions are apparent in both materials. The first transition spans from 0 to 50 °C and the second from 100 to 200 °C.

Kinetics of Adsorption. The effect of temperature on adsorption of NaCl (q = g NaCl/kg foam) by hemicellulose−DTPA−chitosan at pH 3.9, cross-linking ratio 1, and initial concentration of 3 g/L is shown in Figure S8 of the Supporting Information. These results are based on gravimetric measurements of the foams after absorption. The reported values are only the salt interacting with the foam material; extraneous free salt in the free water existing in the foam after the absorption time has not been included in these values. The majority of NaCl uptake of the foams occurs rapidly, within 5 min. The time to reach equilibrium adsorption decreases with increasing temperature. The time to reach 95% of the adsorption equilibrium value is 100, 60, and 35 min at 25, 45, and 55 °C, respectively. Thus, the rate of adsorption dq/dt increases with temperature, indicating a kinetically controlled process. Also, the equilibrium amount of salt adsorption increases with increased temperature. An increase in the initial salt concentration leads to an increase in the adsorption capacity of the salt concentration on foam materials (Figure S9, Supporting Information).

Rate Constant Studies. In order to investigate the mechanism of salt adsorption, the pseudo first-order and pseudo second-order equations were used to model the effects of time, initial salt concentration, and temperature. The correlation coefficients for the first-order kinetic model (Figures S10 and S11, Supporting Information) are low compared to the second-order model fits (Figures S12 and S13, Supporting Information).

The second-order kinetic model[45] is expressed in eq 1 as

$$\frac{t}{q} = \frac{1}{k_2 q_e^2} + \frac{t}{q_e} \quad (1)$$

where q_e and q (g NaCl/kg foam) are the amounts of salt adsorbed on adsorbent at equilibrium and at time t (min), respectively, and k_2 (kg/g per min) is the rate constant of second-order adsorption. The slopes and intercepts of plots of t/q versus t were used to calculate the second-order rate constant k_2 and q_e. The straight lines in plot of t/q versus t show a good agreement of experimental data with the second-order kinetic model for different initial salt concentrations (Figure S12, Supporting Information). The similar straight line agreements are also observed for data at different temperature (Figure S13, Supporting Information). Table 5 lists the

Table 5. Second-Order Adsorption Rate Constants and Calculated and Experimental q_e Values

parameters	q_e exp (g/kg)	second-order kinetic model		
		k_2 (kg/g per min)	q_e cal (g/kg)	R^2
initial concentration (g/L) at T = 25 °C				
3 (g/L)	362.05	1.30 × 10^{-3}	384	1
6 (g/L)	671.53	7 × 10^{-4}	714.28	1
12 (g/L)	3549.3	4.5 × 10^{-4}	3333	1
temperature (°C) at C = 3 g/L				
25 (°C)	373	1.30 × 10^{-3}	384	1
45 (°C)	412	1.52 × 10^{-3}	416	1
55 (°C)	450	2.1 × 10^{-3}	454	1

computed results obtained from the second-order kinetic model. The correlation coefficients for the second-order kinetic model are equal to 1 for almost all the cases. Also, the calculated q_e, values also agree with the experimental data.

Because the foam has a relatively high equilibrium adsorption density q_e, the adsorption rates become very fast, and the equilibrium times are short. Such short equilibrium times coupled with high adsorption capacity indicate a high degree of affinity between salt and the cross-linked foam. Assuming an Arrhenius behavior of the rate constant k_2 on temperature T the activation energy E_a can be determined (eq 2)

$$K_2 = Ae^{-Ea/RT} \quad (2)$$

where R is the gas constant.

The rate constant k_2 at different temperatures (25, 45, 55 °C) was applied to estimate the activation energy of the adsorption of salt on the foams. The slope of plot of ln k_2 versus $1/T$ was used to evaluate E_a, which is 11.86 kJ/mol for the adsorption of NaCl on the foam cross-linked in the temperature range of 25−55 °C. This activation energy is less than the reported value of chitosan with heavy metals,[28] but significant differences exist between these two systems.

Interpretation of Swelling and Salt Sorption Effects. The observed ability of the gel materials described in this article to maintain and even to increase their degree of swelling with aqueous solution with increasing levels of salt and also their unusual ability to take up salt ions from solution can be understood in terms of established principles, including ion exchange, the Donnan equilibrium, osmotic effects, and the so-

called "antipolyelectrolyte effect" describing how salinity can affect the behavior of polyelectrolyte complexes.[29−33]

To account for the observed substantial uptake of saline solution, resulting in a degree of swelling exceeding that obtained in the case of deionized water, two principles should be emphasized. First, both of the types of polyelectrolytes employed in this work are highly hydrophilic due to their multiplicity of ionizable groups. In a sense, the presence of both acidic and basic groups in the same formulation implies two important potential contributions to hydrophilic character. Bound ions within a typical super-absorbent gel, when in the presence of a salt-free continuous aqueous phase, create an imbalance of ionic strength. The bound ionic groups within the gel structure are not matched by a corresponding concentration of ionic groups in the bulk phase, if the salinity is very low. In principle, such an imbalance can be partly resolved either by ion-pair formation,[29,34] swelling of the gel due to osmotic pressure,[29,35,36] or development of relative pressure within the gel.[37,38] A gel that contains both cationic and anionic dissociable groups as a polyelectrolyte complex represents a special case because salt ions tend to weaken the pairwise associations between the acidic and basic groups. Thus, instead of causing progressive collapse of the gel, a moderate level of salt has the potential to increase swelling of such a gel. In the present case, the respective chains are loosely cross-linked with a relatively high content of ionized groups (both positive and negative). A weakening of the ion-pair associates within the polyelectrolyte complex, resulting in dissociation of those bound groups, helps to explain why the observed swelling levels in the presence of salt were able to exceed those that frequently have been reported in the case of super-absorbent hydrogels comprising only one sign of dissociable group.[39] By contrast, in the absence of salt, the polyelectrolyte complexation helps hold the gel in a tight densely packed state and to lessen the importance of the osmotic effects.

Ion exchange is a process by which the counterions associated with bound charges in a gel (or other substrate) are replaced by like-charged ions.[40,41] Situations giving rise to ion exchange can include differences in the affinity of different ions for the sites of adsorption or a higher concentration of the replacing ion.[42] Efforts to take up monovalent species from aqueous solution pose a particular challenge because the binding ability of such ions is typically weak in comparison to multivalent ions of the same charge.[43] The gels considered in this work represent a special case because they were formed by an acid−base interaction, leaving the composition relatively free of counterions within the gel structure.[29,34] When a sufficient concentration of salt, such as NaCl, is added to the biosorbent, the polyelectrolyte complex becomes weakened, allowing monomeric ions such as Na^+ and Cl^- to associate with the bound ionizable groups. This explains why the salt ions will tend to remain in the gel material even if it is squeezed. The overall process can be represented as shown in eq 3, where the dashed line represents the initial ion-pair associations within the polyelectrolyte complex.

$$\mathrm{RCOO^-}\ -\ -\ -^+\ \mathrm{NH_3R'} + \mathrm{NaCl} \rightarrow \mathrm{RCOO^-Na^+} + \mathrm{R'NH_3^+Cl^-} \quad (3)$$

As shown, upon addition of saline solution the initial ion-pair associations can be effectively replaced by interactions with the monomeric ions, taking advantage of the fact that the higher ionic strength conditions tend to loosen the structure of the polyelectrolyte complex. This is a unique behavior relative to typical super-absorbent materials, and one can expect that applications of such behavior will be revealed in future studies.

Heavy Metal Uptake. The adsorption of heavy metal such as nickel(II) and copper(II) and lead(II) were studied at different pH values using switchgrass hemicellulose−DTPA−chitosan foam at initial metal ion concentrations of 5000 PPB (mg/g) and 100 PPB (mg/g) (Table 6). Adjustment of pH was made with 0.1 N HCl and 0.1 N of NaOH solutions.

Table 6. Adsorption of Heavy Metals at Different pH Values Using Switchgrass Hemicellulose−DTPA−Chitosan Foam

	pH 4		pH 5	
Heavy metal	initial metal loading of 5000 PPB (mg/g)	initial metal loading of 100 PPB (mg/g)	initial metal loading of 5000 PPB (mg/g)	initial metal loading of 100 PPB (mg/g)
Pb(II)	2.40	0.20	2.90	0.18
Cu(II)	1.17	0.07	0.95	0.07
Ni(II)	1.20	0.10	1.37	0.14

The results indicate that the maximum uptake of Cu(II) ions takes place at pH 4, while the maximum uptake of Ni(II) ions occurs at pH 5. Moreover, the foam material showed that it has high selectivity for Pb^{2+} and could bind 2.9 mg/g at pH 5. The low level of metal ion uptake by the biosorbent at lower pH values could be attributed to the increased concentration of hydrogen (H^+) ions, which compete along with metals ions for binding sites on the foam. At pH values above the isoelectric point, there is a negative charge on the surface, and the ionic point of ligands such as carboxyl groups are free to promote the interaction with the metals. This would lead to electrostatic attractions between positively charged (metals) and negatively charged binding sites. Note that the adsorption of the divalent ions in Table 6 are much lower than those for the monovalent ions in Table 5.

End of life options need to be further researched but some possibilities are listed here. It is expected that the material could be regenerated using electrolysis as described for chitosan with EDTA by Gyliene et al.[46] Also the material, because it is organic, could be burned in a sanitary combustion process resulting in a concentrated metal stream. For nonhazardous metals, the material could be disposed of in landfills or incorporated into a product that could tolerate it at reasonable loadings, such as paper, concrete, or gypsum wall board, for instance.

■ ASSOCIATED CONTENT

Ⓢ Supporting Information

Isolation of hemicelluloses from the biomass. Effect of DTPA on the properties of hemicelluloses. Reaction between hemicellulose, DTPA, and chitosan. Effect of biosorbent on the conductivity of sodium chloride solution. Scanning electron microscopy of biosorbent after immersion in saline solution. Themo-mechanical tension results of biosorbent. Adsorption kinetics. This material is available free of charge via the Internet at http://pubs.acs.org.

■ AUTHOR INFORMATION

Corresponding Author

*E-mail: richard_venditti@ncsu.edu. Tel: +1 919 515 6185. Fax: +1 919 515 6302.

Notes

The authors declare no competing financial interest.

■ ACKNOWLEDGMENTS

The authors thank the Water Resources Research Institute of the University of North Carolina for its sponsorship of this project.

■ REFERENCES

(1) Carson, R.; Mitchell, R. C. The value of clean water. *Water Resour. Res.* **1993**, *29* (7), 2445−2454.
(2) Elimelech, M.; Philip, W. A. The future of seawater desalination: Energy, technology and the environment. *Science* **2011**, *333* (6043), 712−717.
(3) Greenlee, L.; Lawler, D. F.; Freeman, B. D. Reverse osmosis desalination: Water sources, technology, and today's challenges. *Water Res.* **2009**, *9* (43), 2317−2348.
(4) Imran, A.; Gupta, V. K. Advances in water treatment by adsorption technology. *Nat. Protoc.* **2006**, *1* (6), 2661−2667.
(5) Netzer, A.; Hughes, D. E. Adsorption of copper, lead and cobalt by activated carbon. *Water Res.* **1984**, *18* (8), 927−933.
(6) Li, L.; Quinlivan, P. A.; Knappe, D. R. U. Effects of activated carbon surface chemistry and pore structure on the adsorption of organic contaminants from aqueous solution. *Carbon* **2002**, *40* (12), 2085−2100.
(7) Madhava Rao, M.; Ramesh, A.; Purna Chandra Rao, G.; Seshaiah, K. Removal of copper and cadmium from the aqueous solutions by activated carbon derived from *Ceiba pentandra* hulls. *J. Hazard. Mater.* **2006**, *129* (1−3), 123−129.
(8) Singh, K. P.; Mohan, D.; Sinha, S.; Tondon, G. S.; Gosh, D. Color removal from wastewater using low-cost activated carbon derived from agricultural waste material. *Ind. Eng. Chem. Res.* **2003**, *42* (9), 1965−1976.
(9) Gabrielli, I.; Gatenholm, P.; Glasser, W. G.; Jain, R. K.; Kenne, L. Seperation, characterization and hydrogel-formation of hemicellulose from aspen wood. *Carbohydr. Polym.* **2000**, *43* (4), 367−374.
(10) Salam, A.; Venditti, R. A.; Pawlak, J. J.; El-tahlawy, K. Crosslinked hemicellulose citrate−chitosan aerogel foams. *Carbohydr. Polym.* **2011**, *84*, 1221−1229.
(11) Karaaslan, M. A.; Tshabalal, A. A.; Buschle-Diller, G. Wood hemicellulose chitosan based semi-interpenetrating network hydrogels: Mechanical, swelling and controlled drug release properties. *Bioresources* **2010**, *5* (2), 1036−1054.
(12) Bai, L.; Hu, H.; Xu, J. Influences of configuration and molecular weight of hemicelluloses on their paper-strenthening effects. *Carbohydr. Polym.* **2012**, *88* (4), 1258−1263.
(13) Fang, J. M.; Sun, R. C.; Tomkinson, J.; Fowler, P. Acetylation of wheat straw hemicellulose B in a new non-aqueous swelling system. *Carbohydr. Polym.* **2000**, *41* (4), 379−387.
(14) Lindblad, M. S.; Ranucci, E.; Albertsson, A. C. Biodegradable polymers from renewable sources. New hemicellulose-based hydrogels. *Macromol. Rapid Commun.* **2001**, *22* (12), 962−967.
(15) Salam, A.; Pawlak, J. J.; Venditti, R. A.; El-tahlawy, K. Incorporation of carboxyl groups into xylan for improved absorbency. *Cellulose* **2011**, *18*, 1033−1041.
(16) Ma, Z.; Li, Q.; Yue, Q.; Gao, B.; Xu, X.; Zhong, Q. Synthesis and characterization of a novel super-absorbant based on wheat straw. *Bioresour. Technol.* **2011**, *102* (3), 2853−2858.
(17) Gao, D.; Heimann, R. B. Structure and mechanical properties of superabsorbent poly(acrylamide)-montmorillonite composite hydrogels. *Polym. Gels Networks* **1993**, *1* (4), 225−246.
(18) Guilherme, M. R.; Campese, G. M.; Radovanivic, E.; Rubira, A. F.; Feitosa, J.P. A.; Muniz, E. C. Morphology and water affinity of superabsorbent hydrogels composed of methacrylated cashew gum and acrylamide with good mechanical properties. *Polymer* **2005**, *46*, 7867−7873.
(19) Dutkiewicz, J. K. Superabsorbent materials from shellfish waste: A review. *J. Biomed. Mater. Res.* **2002**, *63* (3), 373−381.
(20) Gabreielii, I.; Gatenholm, P. Preparation and properties of hydrogels based on hemicellulose. *J. Appl. Polym. Sci.* **1998**, *69* (8), 1661−1667.
(21) Repo, E.; Warchol, J. K.; Kurniawan, T. A.; Mika, E.; Sillanpaa, T. Adsorption of Co(II) and Ni(II) by EDTA- and/or DTPA-modified chitosan: Kinetic and equilibrium modeling. *Chem. Eng. J.* **2010**, *161* (1−2), 73−82.
(22) Saha, T. K.; Ichikawa, H.; Fukumori, Y. Gadolinium diethylenetriaminopentaacetic acid-loaded chitosan microspheres for gadolinium neutron-capture therapy. *Carbohydr. Res.* **2006**, *341* (17), 2835−2841.
(23) Ayoub, A.; Venditti, R. A.; Pawlak, J. J.; Sadeghifar, H.; Salam, A. Development of an acetylation reaction of switchgrass hemicellulose in ionic liquid without catalyst. *Ind. Crops Prod.* **2013**, *44*, 306−314.
(24) Kim, S. B.; Lee, Y. Y. Fractionation of herbaceous biomass by ammonia-hydrogen peroxide percolation treatment. *Appl. Biochem. Biotechnol.* **1996**, *57* (1), 147−156.
(25) Biomass Feedstock Composition and Property Database, 2006. NERL (National Renewable Energy Laboratories). http://www1.eere.energy.gov/biomass/biomass_feedstocks.html (accessed June 20, 2013).
(26) Lange, J. P. Lignocellulose conversion: An interaction to chemistry, process and economics. *Biofuels, Bioprod. Biorefin,* **2007**, *1* (1), 39−48.
(27) Sun, R. C.; Hughes, S. Fractional extraction and physic-chemical characterization of hemicellulose and cellulose from sugar beet pulp. *Carbohydr. Polym.* **1999**, *36* (4), 293−299.
(28) Babel, S.; Kurniawam, T. A. Low-cost adsorbents for heavy metals uptake from contaminated water: A review. *J. Hazard. Mater.* **2003**, *B* (97), 219−243.
(29) Baker, J. P.; Blanch, H. W.; Prausnitz, J. M. Swelling properties of acrylamide-based ampholytic hydrogels: Comparison of experimental with theory. *Polymer* **1995**, *36* (5), 1061−1069.
(30) Valencia, J.; Pierola, I. F. Interpretation of the polyelectrolyte and antipolyelectrolyte effects of poly)N-vinylimidazole-co-sodium styrenesulfonate) hydrogels. *J. Polym. Sci., Part B: Polym. Phys.* **2007**, *45* (13), 1683−1693.
(31) Dogu, S.; Kilic, M.; Okay, O. Collapse of acrylamide-based polyampholyte hydrogels in water. *J. Appl. Polym. Sci.* **2009**, *113* (3), 1375−1382.
(32) Wang, J.; Xu, L.; Li, C. C.; Yue, Z. Y.; Zhai, M. L.; Li, J. Q. Antipolyelectrolyte swelling of amphiphilic hydroxypropyl methylcellulose phthalate gels. *Colloids Surf., A* **2010**, *356*, 89−96.
(33) Gawel, K.; Gao, M.; Stokke, B. T. Impregnation of weakly charged anionic microhydrogels with cationic polyelectrolytes and their swelling properties monitored by a high resolution interferometric technique. Transformation from a polyelectrolyte to a polyampholyte hydrogel. *Eur. Polym. J.* **2012**, *48* (11), 1949−1959.
(34) Michaels, A. S. Polyelectrolyte complexes. *Indust. Eng. Chem.* **1965**, *57* (10), 32−40.
(35) Chiu, H. C.; Lin, Y. F.; Hung, S. H. Equilibrium swelling of copolymerized acrylic acid-methacrylated dextran networds: Effects of pH and neutral salt. *Macromolecules* **2002**, *35* (13), 5235−5242.
(36) Wang, D.; Song, Z. Q.; Sahng, S. B. Characterization and biodegradability of amphoteric superabsorbent polymers. *J. Appl. Polym. Sci.* **2008**, *107* (6), 4116−4120.
(37) Scallan, A. M.; Tigerström, A. G. Swelling and elasticity of the cell walls of pulp fibers. *J. Pulp Paper Sci.* **1992**, *18* (5), J188−J193.
(38) Buchholz, F. L.; Pesce, S. R.; Powell, C. L. Deswelling stresses and reduced swelling of superabsorbent polymer in composites of fiber and superabsorbent polymers. *J. Appl. Polym. Sci.* **2005**, *98* (6), 2493−2507.
(39) Athawale, V. D.; Lele, V. Recent trends in hydrogels based on starch-graft-acrylic acid: A review. *Starch/Staerke* **2001**, *53* (1), 7−13.
(40) Zhong, L. X.; Peng, X. W.; Yang, D.; Sun, R. C. Adsorption of heavy metals by a porous bioadsorbent from lignocellulosic biomass reconstructed in an ionic liquid. *J. Agric. Food Chem.* **2012**, *60* (22), 5621−5628.

(41) Hubbe, M. A.; Hasan, S. H.; Ducoste, J. J. Cellulosic substrates for removal of pollutants from aqueous systems: A review. 1. Metals. *Bioresources 6* (2), 2161-2287

(42) Hanninen, K. R.; Murtomaki, L. S.; Kaukonen, A. M.; Hirvonen, J. T. The effect of valence on the ion-exchange process: Theoretical and experimental aspects on compound binding/release. *J. Pharm. Sci.* **2007**, *96* (1), 117−131.

(43) Rudie, A. W.; Ball, A.; Patel, N. Ion exchange of H^+, Na^+, Mg^{2+}, Ca^{2+}, Mn^{2+}, and Ba^{2+} on wood pulp. *J. Wood Chem. Technol.* **2006**, *26* (3), 259−27.

(44) Venditti, R.; Gillham, J. K. Anomalous behavior of thermosetting systems after cure vs chemical conversion: A normalized conversion-temperature-property diagram. *J. Appl. Polym. Sci.* **1995**, *56*, 1687−1705.

(45) Azizian, S. Kinetics models of sorption: A theoretical analysis. *J. Colloid Interface Sci.* **2004**, *276*, 47−52.

(46) Gyliene, O.; Nivinskiene, O.; Razmute, I. Copper (II)-EDTA sorption onto chitosan and its regeneration applying electrolysis. *J. Hazard Mater.* **2006**, *137* (3), 1430−1437.